



Gas-phase catalytic growth of single-walled carbon nanotubes from carbon monoxide

Pavel Nikolaev, Michael J. Bronikowski, R. Kelley Bradley, Frank Rohmund,
Daniel T. Colbert, K.A. Smith, Richard E. Smalley *

Rice University, The Center for Nanoscale Science and Technology - MS 100, 6100 Main, Houston, TX 77005-1892, USA

Received 8 July 1999

Abstract

Single-walled carbon nanotubes (SWNTs) have been produced in a gas-phase catalytic process. Catalysts for SWNT growth form in situ by thermal decomposition of iron pentacarbonyl in a heated flow of carbon monoxide at pressures of 1–10 atm and temperatures of 800–1200°C. The SWNT yield and diameter distribution can be varied by controlling the process parameters, and SWNTs as small as 0.7 nm in diameter, the same as that of a C₆₀ molecule, have been generated. This process shows great promise for bulk production of carbon nanotubes. © 1999 Elsevier Science B.V. All rights reserved.

1. Introduction

Single-walled carbon nanotubes (SWNTs) exhibit many unique and useful physical and chemical properties [1]. Demonstrated methods for producing SWNTs involve laser vaporization of metal-doped carbon targets [2], arc evaporation of metal-doped carbon electrodes [3], and decomposition of carbon-containing molecules such as C₂H₄ and CO [4] and CH₄ on supported nanometer-sized metal particles that serve as catalysts for SWNT growth [5]. All of these methods produce SWNTs in milligram to gram quantities in a few hours. However, many potential applications of SWNTs require kilogram to ton quantities.

A continuous-flow synthetic method, in which SWNTs are grown (and separated) in a flowing gaseous feedstock mixture, could produce SWNTs in large quantities. Such schemes would involve introducing into the feedstock flow stream nanometer-size catalyst particles on which the individual tubes nucleate and grow. The catalyst particles could be either pre-made or produced in situ by the introduction of metal-containing species into the flow and their subsequent condensation into appropriately sized clusters. The latter technique is especially convenient, because metal can be introduced in the form of volatile organometallic molecules.

Many groups have investigated gas-phase continuous-flow production of carbon fibers. These studies typically involve passing a mixture of carbon source gas and organometallic catalyst precursor molecules through a heated furnace. The organometallics decompose and react, forming clusters on which carbon

* Corresponding author. Fax: +1-713-285-5320; e-mail: res@cnst.rice.edu, web: <http://cnst.rice.edu/reshome.html>

fibers nucleate and grow. Tibbets et al. have reported gas-phase synthesis of carbon fibers in heated flowing mixtures of methane or hexane with organometallics such as iron pentacarbonyl ($\text{Fe}(\text{CO})_5$) [6] and ferrocene (dicyclopentadienyl iron, $\text{Fe}(\text{Cp})_2$) [7]. Rao and co-workers [8–10] have investigated the catalytic growth of carbon nanotubes in gas phase, both by direct pyrolysis of ferrocene and other metallocenes and by catalytic decomposition of hydrocarbons or carbon monoxide in the presence of metallocenes or $\text{Fe}(\text{CO})_5$. In two of these studies, this group reported production of SWNTs from mixtures of $\text{Fe}(\text{CO})_5$ with acetylene [8] and benzene [10]. Very recently, Dresselhaus and co-workers have reported the production of SWNTs in a heated flow of benzene and ferrocene [11,12].

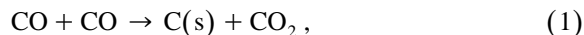
To date, all investigations reporting gas-phase continuous-flow production of SWNTs have relied on hydrocarbons as the carbon source molecule for tube growth. However, hydrocarbons pyrolyze readily on most surfaces heated above 600–700°C (temperatures required for growth of SWNTs), forming graphitic deposits or amorphous carbon. Nanotubes grown in heated flows of gaseous hydrocarbons often show substantial amorphous carbon overcoating, which would need to be removed in subsequent processing steps. One may anticipate that such effects would complicate efforts to scale up production methods using hydrocarbon feedstocks.

We report here the catalytic production of SWNTs in a continuous-flow gas-phase process using CO as the carbon feedstock and $\text{Fe}(\text{CO})_5$ as the iron-containing catalyst precursor. We find that both the yield of SWNT material and the diameters of the nanotubes produced can vary over a wide range, depending on the conditions and flow-cell geometry used. In particular, we have succeeded in producing SWNTs with diameters of 0.7 nm, which are expected to be the smallest achievable chemically stable SWNTs [1]. This process (or variations of it) should be scalable for bulk SWNT production.

2. Experimental

We have produced SWNTs by flowing CO mixed with a small amount of $\text{Fe}(\text{CO})_5$ through a heated

reactor (Fig. 1). The products of $\text{Fe}(\text{CO})_5$ thermal decomposition (probably $\text{Fe}(\text{CO})_n$, $n = 0-4$) react to produce iron clusters in gas phase. These clusters act as nuclei upon which SWNTs nucleate and grow: solid carbon is produced by CO disproportionation (the Boudouard reaction):



which occurs catalytically on the surface of the iron particles. These particles also promote the formation of the tube's characteristic graphitic carbon lattice.

The flow cell apparatus consists of a 1" (2.54 cm) OD thick-walled quartz flow tube contained within a tube furnace, through which reactant gases are flowed. The tube section inside the furnace was maintained between 800 and 1200°C, while the tube entrance and exit were maintained at room temperature. We found that the rate at which the reactant gases were heated had substantial effects on the amount and quality of SWNTs produced. In some experiments the CO and $\text{Fe}(\text{CO})_5$ were introduced through a water-cooled injector positioned inside the quartz tube, which maintained the gases at low temperature until they were injected into the furnace, resulting in rapid heating. Around the exit of this injector could be positioned a circle of narrow-gauge needles through which preheated CO was passed at high flow rate to mix with the cool flow emerging from the injector, further increasing the heating rate of the injected gas. The CO sprayed from this 'showerhead' mixer was preheated by passing through a spiral heat exchanger positioned within the furnace.

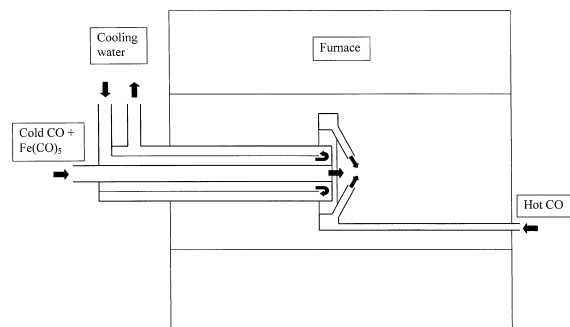


Fig. 1. Layout of CO flow-tube reactor, showing water-cooled injector and 'showerhead' mixer.

Our gas mixture consisted of CO (1–10 atm flowing at 1–2 standard liters per minute) dosed with a small amount (0–25 mTorr) of gaseous $\text{Fe}(\text{CO})_5$. Dosing was accomplished by passing a measured fraction of the CO stream through a $\text{Fe}(\text{CO})_5$ -filled bubbler maintained at 0°C . This produced a partial pressure of $\text{Fe}(\text{CO})_5$ equal to its vapor pressure of ~ 7 Torr, and the partial pressure of $\text{Fe}(\text{CO})_5$ was subsequently reduced by diluting with additional CO before its introduction into the flow cell. Commercial CO will always contain a few ppm of $\text{Fe}(\text{CO})_5$ as a contaminant, which we filtered out using an in-line catalytic purifier (Oxyzorb, Matheson) prior to introduction into our flow system. Alternately, this small ‘background’ concentration of $\text{Fe}(\text{CO})_5$ was used directly in experiments with high CO pressure and/or low $\text{Fe}(\text{CO})_5$ concentration because the bubbler was found to be unreliable under these conditions. The concentration of background $\text{Fe}(\text{CO})_5$ in the CO stream, typically 2–10 ppm, was determined by measuring the total amount of iron deposited in the reactor. In control experiments using no $\text{Fe}(\text{CO})_5$ (with the catalytic purifier in use), no iron or carbon reaction products were observed.

Flow of CO/ $\text{Fe}(\text{CO})_5$ mixtures through the heated reactor resulted in black deposits on the walls of the quartz tube outside the furnace. These deposits consisted of SWNTs and iron particles apparently overcoated with carbon. Material was collected and weighed, and analyzed using transmission electron microscopy (TEM), scanning electron microscopy (SEM), energy-dispersive X-ray spectroscopy (EDX), and thermogravimetric analysis (TGA).

3. Results

Gas-phase iron pentacarbonyl will decompose rapidly at 250°C [13]. Reaction (1) occurs at a significant rate only at temperatures above 500°C [14]. One may thus anticipate that the rate at which the gas mixture is heated through the temperature range of 200 – 500°C will be important in determining the outcome of this process: too slow a heating rate could allow the forming Fe clusters to grow too large or encounter and stick to the quartz tube wall before they reach the temperature required for reaction (1) to proceed, thus preventing SWNT nucleation and

growth in the gas phase. This was confirmed in initial experiments conducted without the cooled injector. In these experiments, 6.5 atm of unpurified CO was flowed directly through the quartz tube heated to 850°C . We determined that the CO contained 4–5 ppm of $\text{Fe}(\text{CO})_5$, giving a $\text{Fe}(\text{CO})_5$ concentration of 20–25 mTorr. When the flow velocity in the region of transition from room temperature to SWNT growth temperature (~ 10 cm long) was around 10–20 cm/s, we found that SWNTs were produced and deposited as thin mats or films on the cold parts of the quartz tube. When the flow velocity was slower¹, 0.5–1 cm/s, no SWNTs were formed. Fig. 2 shows TEM and SEM images of the SWNT material from these experiments. Approximately 3.6 mg of material was produced in 16 h of gas flow at 1500 sccm. EDX and TGA showed that the material contained 45% of iron atoms, or 75% iron by weight.

Much more rapid heating of the CO/ $\text{Fe}(\text{CO})_5$ mixture was achieved using the cooled injector, and this setup was used to study the dependence of SWNT production on temperature and pressure. In these experiments, CO containing 5 ppm of $\text{Fe}(\text{CO})_5$ was flowed through the heated reactor tube at 1000 sccm for 5–15 h. Nanotube containing material was deposited on the walls of the quartz tube and on a filter positioned downstream of the reactor. This material was collected, weighed, and the mass fraction of carbon was determined by TGA. TEM observations of the product material suggest that most of the carbon was present as SWNTs, rather than other forms such as amorphous carbon. TEM images also gave the diameter distributions of the product SWNTs. Very few tube ends were observed, implying that the tubes are long compared to their width: we estimate average tube length of ~ 1 μm , based on the number of tube ends observed.

Table 1 lists the rate of SWNT production vs. temperature at 10 atm. We found that the highest production rate was achieved at our furnace’s highest available temperature, 1200°C . We next investigated

¹ This experiment was performed with the furnace positioned vertically, which forced a uniform gas flow. In the former experiment the furnace was positioned horizontally, and gas was drawn into the furnace much faster (10–20 cm/s) due to formation of a convection cell.

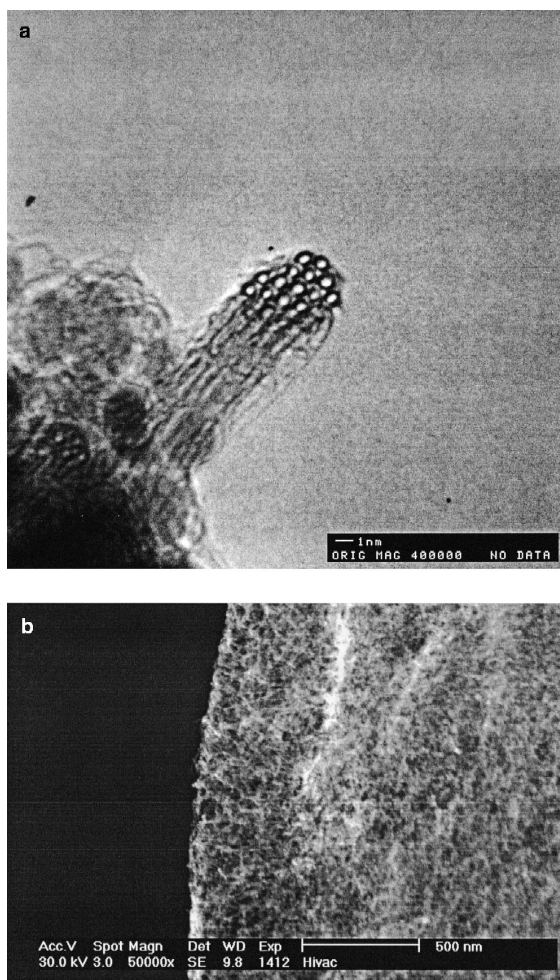


Fig. 2. (a) SEM image of SWNT ropes produced in a flow of CO (6.5 atm) and $\text{Fe}(\text{CO})_5$ (5 ppm) through the flow-tube apparatus heated to 850°C. (b) TEM image of nanotubes produced in a flow of CO (6.5 atm) and $\text{Fe}(\text{CO})_5$ (5 ppm) heated to 850°C, showing nanotube rope cross-section.

SWNT production rate vs. pressure at 1200°C, where the CO pressure was varied from 1 to 10 atm and the relative concentration of $\text{Fe}(\text{CO})_5$ was maintained at

Table 1

Temperature (°C)	Production rate (mg/h)	SWNT yield (mole%)	SWNT yield (wt.%)
850	0.68	73	37
1000	1.00	71	34
1200	1.24	79	44

Table 2

Pressure (atm)	Production rate (mg/h)	SWNT yield (mole%)	SWNT yield (wt.%)
1	1.16	61	25
3	1.38	67	30
10	1.24	79	44

5 ppm. Again we found that production rate increased with increasing pressure up to the maximum pressure we could achieve, 10 atm. Table 2 lists the SWNT production rate vs. CO pressure. We also observed that the diameters of the product SWNTs varied as reaction conditions were varied. Fig. 3 shows the diameter distributions observed at various pressures. The product SWNTs consistently showed smaller diameters as pressure was increased. Reaction at 10 atm gave tubes as small as 0.7 nm in diameter, which is about the diameter of a C_{60} molecule.

Experiments with the cooled injector alone using higher $\text{Fe}(\text{CO})_5$ concentrations did not give additional nanotube material. Rather, iron in excess of 5 ppm merely formed additional iron particles mixed in with the product material. This inefficient use of available iron could result from too small a heating rate of the CO/ $\text{Fe}(\text{CO})_5$ mixture. Therefore the 'showerhead' mixer (Fig. 1) was implemented to achieve even faster heating of the injected gases. In experiments with this mixer the CO pressure was maintained at 3 atm rather than 10 atm in order to achieve higher gas flow velocities. The CO/ $\text{Fe}(\text{CO})_5$ mixture was flowed through the cooled injector at 1000 sccm, while hot gas (pure CO) was sprayed from the mixer at 5000 sccm. All showerhead mixer experiments were carried out at 1200°C.

Using this setup we were able to utilize somewhat higher $\text{Fe}(\text{CO})_5$ concentrations in the CO. $\text{Fe}(\text{CO})_5$ concentrations of 8 ppm gave SWNT production rates of up to 15 mg/h. The showerhead also led to more efficient use of the available iron: 8 ppm of $\text{Fe}(\text{CO})_5$ gave product material containing only 7 mole% iron, compared to 31 mole% obtained using 5 ppm $\text{Fe}(\text{CO})_5$ with the cooled injector alone. The diameter distributions of the SWNTs from the showerhead configuration were similar to those from the cooled injector alone (Fig. 3). Clearly, the rate of heating of the CO/ $\text{Fe}(\text{CO})_5$ mixture has a substan-

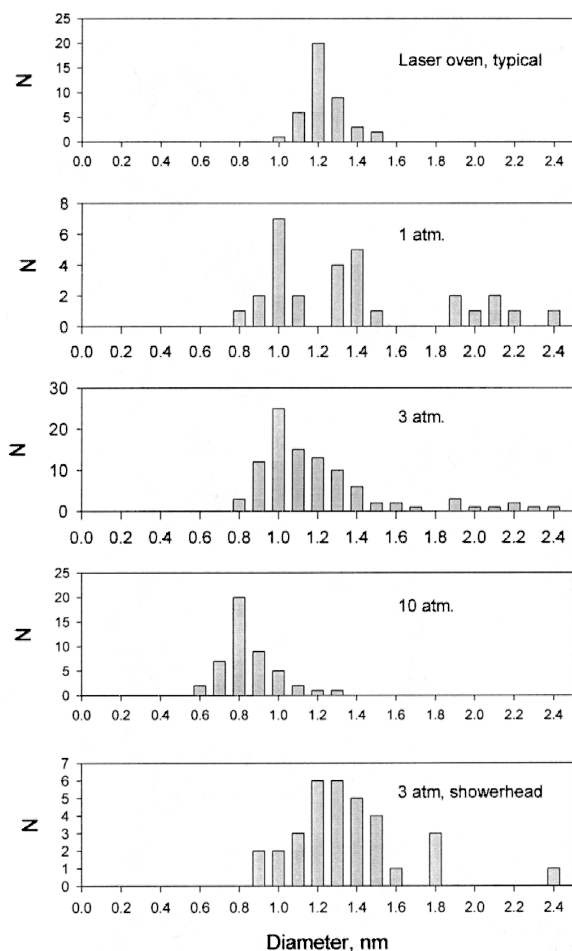


Fig. 3. Diameter distributions of SWNT produced at 1200°C, at various CO pressures.

tial effect on the SWNT material produced. Fig. 4 shows TEM images of the SWNT material produced using the cooled injector with the showerhead mixer. Note from the TEM images in both Figs. 2 and 4 that SWNTs produced by this process are essentially free of amorphous carbon overcoating.

One disadvantage of CO over hydrocarbons as a carbon feedstock is that, at a given temperature and pressure, CO disproportionation is much slower than hydrocarbon thermal decomposition. We therefore performed additional experiments in which a small amount of methane was added to the CO flow to increase the amount of carbon available for SWNT

growth. Small amounts of methane (0.7% by volume) produced clean nanotubes in increased yields: the yield with methane was 20 mg/h of material containing 5 at.% iron, vs. 15 mg/h of 7% iron material produced under identical conditions without methane. However, higher CH_4 concentrations (1.4%) gave nanotubes with significant amorphous

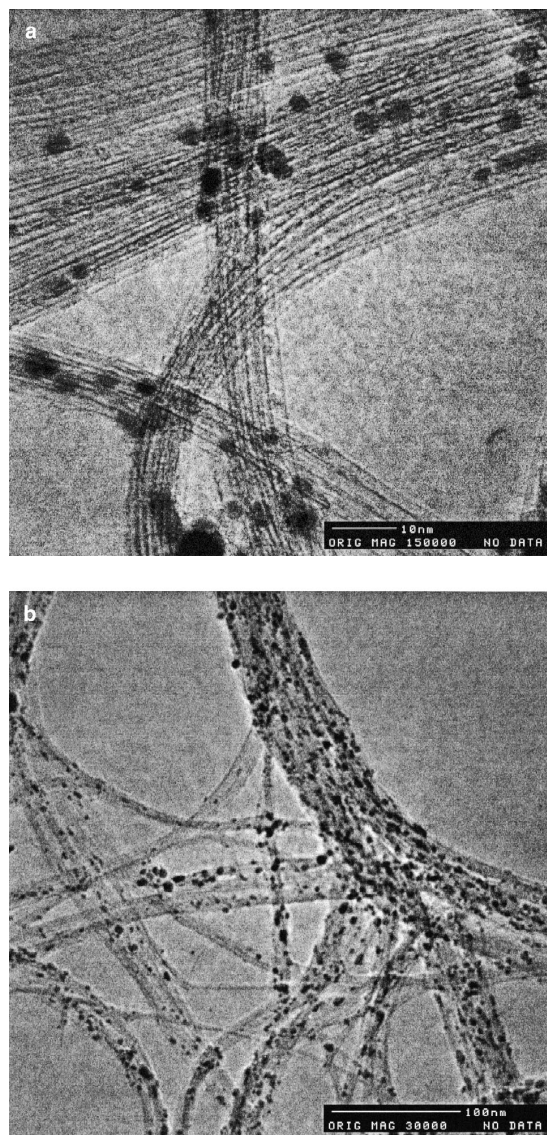


Fig. 4. (a) Low-magnification TEM image of SWNT material produced using the cooled injector with showerhead mixer. Conditions: 3 atm CO with 8 ppm of $\text{Fe}(\text{CO})_5$, 1200°C. (b) High-magnification TEM image of SWNT material in (a).

overcoating unless the reaction temperature was lowered from 1200 to 1100°C.

4. Discussion

We propose a model for gas-phase nanotube growth in which metal clusters form first, then nucleate and grow SWNTs. Metal clusters initially form by aggregation of iron atoms from the decomposition of $\text{Fe}(\text{CO})_5$. Clusters grow by collision with additional metal atoms and other clusters, eventually reaching a diameter comparable to that of a SWNT, 0.7–1.4 nm, corresponding to 50–200 iron atoms. By the time they reach that size, CO can disproportionate on the surface of such clusters via reaction (1) to yield solid carbon, and SWNTs will nucleate and grow from them by the ‘Yarmulke’ mechanism [15]. That is, a hemifullerene cap forms on the partially carbon-coated particle, lifts off, and additional carbon atoms are continuously added to the edge of the cap, forming a hollow tube of constant diameter which grows away from the particle. As with supported catalysts [4,15], one expects that the diameter of the nanotube will reflect the size of the catalytic particle *at the time of tube nucleation*. The observed SWNT diameter distribution should thus correspond to the size distribution of the catalyst particles that spawn nanotubes. The smallest SWNTs we ever see are ~ 0.7 nm in diameter, the size of a C_{60} molecule. Since in this model growing tubes will be capped with a hemifullerene (one half of a spherical fullerene molecule), our observation is consistent with the fact that C_{60} is the smallest stable fullerene: SWNTs cannot nucleate on smaller Fe particles because no stable end cap can form. Delays in cap formation and lift-off will allow the Fe particle to accumulate more iron and grow larger so that, if a SWNT does eventually nucleate it will have a larger diameter. This explains why we observe smaller SWNT diameters and narrower diameter distributions as CO pressure is increased: higher CO pressure leads to faster CO disproportionation, giving more C atoms on each Fe particle and faster (earlier) SWNT nucleation relative to continued particle growth. Also, more SWNTs are produced, both in absolute terms and relative to the mass of iron catalyst consumed, as temperature and pressure are

increased. Reaction (1) should be faster as these parameters are increased.

Of central importance is the mechanism by which nanotube growth ceases. The particles in the product material are 5–10 nm in diameter, much larger than SWNT diameters, suggesting that the particles continue to grow even after nucleating a tube. The additional accreting iron atoms could come from either direct gas-phase collisions with other atoms or clusters, or by adsorption of Fe atoms onto the growing tube and their diffusion to the particle at the end. Note that we never see nanotubes with non-constant diameter: apparently, once the SWNT is nucleated, additional carbon atoms can only add to the existing structure with its fixed diameter. As long as the catalytic particle is about the same size as the nanotube growing from it, it is energetically more favorable for carbon to add to the nanotube than to form a layer overcoating the catalyst particle. As the catalyst particle becomes larger, however, the strain energy of the overcoating layer becomes smaller, and formation of a graphitic overcoat is favored [4]. Thus the catalyst particle ultimately overcoats, terminating further nanotube growth. The particle might separate from the nanotube end (which would seal over), but most likely the particle/nanotube pair remain physisorbed together.

We estimate a product SWNT length of $\sim 1 \mu\text{m}$ ($\sim 10^5$ carbon atoms), based on the frequency with which tube ends are observed in TEM images. The particles in our product material, 5–10 nm wide, will contain 10^4 – 10^5 iron atoms. Our observed C:Fe mole ratios of between 5:1 and 10:1 thus imply that the number of nanotubes in our product material is approximately equal to the number of iron particles, suggesting that the particles in the product material are the same ones that nucleated the nanotubes when they were smaller.

Even under our best conditions the ratio of SWNTs produced to iron consumed is not very high. Ideally, every iron atom would be part of a cluster of 50–200 atoms that spawns its own nanotube. If, on average, a 100-atom iron cluster spawns and grows a $1 \mu\text{m}$ tube, we would see product material with a C:Fe mole ratio of 1000:1. Our observed C:Fe ratio of about 10:1, thus implies that most of the iron is consumed not in forming nuclei, but in the continued growth of particles after SWNT nucleation: ongoing

Fe accretion is faster than formation of initial tube-nucleating clusters. Note that the 10:1 carbon-to-iron ratio is maintained over a wide range of experimental parameters and is approximately the same as that observed in the laser-oven apparatus [2].

The yield of carbon to iron can be increased in either of two ways. If a growing SWNT ‘lives’ for only a certain time before growth ceases due to excess iron accretion followed by overcoating, one may be able to increase yield simply by operating at higher CO pressures, which reduce the relative amount of catalyst present and may increase the rate of reaction (1). Another strategy is to increase the fraction of the metal that goes into small, tube-nucleating clusters relative to the fraction that accretes onto active catalyst clusters. If this can be achieved, more of the iron will contribute to initiating tube growth, and less to ending it. If initial thermal dissociation of $\text{Fe}(\text{CO})_5$ is the rate-limiting step in producing Fe clusters, one might speed up the process using higher temperatures or using non-thermal means to decompose the $\text{Fe}(\text{CO})_5$, e.g. laser photolysis. All of these possibilities are currently being explored.

5. Conclusions

We have demonstrated a technique for catalytic production of single-walled nanotubes in gas phase. Our flow reactor uses carbon monoxide as the carbon feedstock and gaseous iron pentacarbonyl as the metal-particle catalyst precursor. Unlike methods involving hydrocarbon feedstocks, our method results in no amorphous carbon overcoating on the product nanotubes. Nanotubes as small as 0.7 nm in diameter have been produced, and the size and diameter distribution of the nanotubes produced can be roughly selected by controlling the pressure of CO in which the reaction occurs. Highest yields (and narrowest tubes) were produced at the highest accessible temperature and pressure, 1200°C and 10 atm, respectively. This process has advantages over other SWNT

production methods: it is a continuous-flow process rather than a batch process, and should be able to be scaled up to produce SWNTs in much larger quantities.

Acknowledgements

This work was supported by the National Aeronautics and Space Administration, the Texas Advanced Technology Program, and the Robert A. Welch Foundation.

References

- [1] B.I. Yakobson, R.E. Smalley, *Am. Sci.* 85 (1997) 324.
- [2] A. Thess, P. Nikolaev, H.J. Dai, P. Petit, J. Robert, C.H. Xu, Y.H. Lee, S.G. Kim, A.G. Rinzler, D.T. Colbert, G.E. Scuse-ria, D. Tomanek, J.E. Fischer, R.E. Smalley et al., *Science* 273 (1996) 483.
- [3] C. Journet, W.K. Maser, P. Bernier, A. Loiseau, M.L. Delachapelle, S. Lefrant, P. Deniard, R. Lee, J.E. Fischer, *Nature (London)* 388 (1997) 756.
- [4] J.H. Hafner, M.J. Bronikowski, B.R. Azamian, P. Nikolaev, A.G. Rinzler, D.T. Colbert, K.A. Smith, R.E. Smalley, *Chem. Phys. Lett.* 296 (1998) 195.
- [5] J. Kong, A.M. Cassel, H. Dai, *Chem. Phys. Lett.* 292 (1998) 567.
- [6] G.G. Tibbetts, C.A. Bernardo, D.W. Gorkiewicz, R.L. Alig, *Carbon* 32 (1994) 569.
- [7] G.G. Tibbetts, D.W. Gorkiewicz, R.L. Alig, *Carbon* 31 (1993) 809.
- [8] B.C. Satishkumar, A. Govindaraj, R. Sen, C.N.R. Rao, *Chem. Phys. Lett.* 293 (1998) 47.
- [9] R. Sen, A. Govindaraj et al., *Chem. Phys. Lett.* 267 (1998) 276.
- [10] R. Sen, A. Govindaraj et al., *Chem. Mater.* 9 (1997) 2078.
- [11] H.M. Cheng, F. Li, G. Su, H.Y. Pan, L.L. He, X. Sun, M.S. Dresselhaus, *Appl. Phys. Lett.* 72 (1998) 3282.
- [12] H.M. Cheng, F. Li, X. Sun, S.D.M. Brown, M.A. Pimenta, A. Marucci, G. Dresselhaus, M.S. Dresselhaus, *Chem. Phys. Lett.* 289 (1998) 602.
- [13] D. Nicholls, in: J.C. Bailar, Jr., H.J. Emeleus, R. Nyholm, A.F. Trotman-Dickenson (Eds.), *Comprehensive Inorganic Chemistry*, vol. 3, Pergamon, Oxford, 1973, p. 990.
- [14] G.D. Renshaw, C. Roscoe, P.L. Walker Jr., *J. Catal.* 18 (1970) 164.
- [15] H.J. Dai, A.G. Rinzler, P. Nikolaev, A. Thess, D.T. Colbert, R.E. Smalley, *Chem. Phys. Lett.* 260 (1996) 471.